CHAPTER 2

Materials and Methods

2.1 Introduction

This chapter provides an overview of the materials and experimental methods for the synthesis and applications of fluorescent carbon quantum dots (CQDs), which have been used in sensing applications. Additionally, this chapter discusses various modern characterization techniques, such as Fourier Transform Infrared (FTIR) Spectroscopy, UV-visible spectroscopy, Fluorescence Spectroscopy, Transmission Electron Microscopy (TEM), Energy-Dispersive X-Ray Spectroscopy (EDAX), Selected Area Electron Diffraction Pattern (SAED), and X-Ray Photoelectron Spectroscopy (XPS). Further, various applications of CQDs are discussed briefly for detection assays of H_2O_2, Ascorbic acid, Picric acid and chlorpyrifos. The present chapter also includes the biocompatibility and cell viability in HeLa cervical cancer cells. Moreover, it discusses the application of CQDs as peroxidase-like activity as well as the determination of fluorescence quantum yield, Stern-Volmer plot, and detection limit. As discussed in this chapter, stock solutions are prepared for analyses of different analytes.

2.2 Materials

In this study, an economically viable and energy efficient route for the synthesis of CQDs has been established. This study synthesized CQDs from chemical and biological precursors for detecting H_2O_2, Ascorbic acid, Picric acid and chlorpyrifos. In the application part of the study, AR grade chemicals were used without any modification and listed in Table 2.1. Ultrapure water was used throughout the entire study as a solvent.

Table 2.1 List of Chemicals

S. No.	Name	Chemical formula	Physical state	Manufacturer
1	Ferric Chloride	$FeCl_3$	Solid	SD Fine-Chem Ltd.
2	Manganese Chloride	$MnCl_2$	Solid	SD Fine-Chem Ltd.
3	Lead Chloride	$PbCl_2$	Solid	SD Fine-Chem Ltd.
4	Iron (II) Chloride Tetrahydrate	$FeCl_2.4H_2O$	Solid	SD Fine-Chem Ltd.
5	Cobaltous Nitrate	$Co(NO_3)_2.6H_2O$	Solid	SD Fine-Chem Ltd.
6	Arsenic tri-oxide	As_2O_3	Solid	SD Fine-Chem Ltd.

7	Calcium Chloride	$CaCl_2$	Solid	SD Fine-Chem Ltd.
8	Nickel Chloride	$NiCl_2.6H_2O$	Solid	SD Fine-Chem Ltd.
9	Zinc Nitrate	$Zn(NO_3)_2$	Solid	SD Fine-Chem Ltd.
10	Cadmium Nitrate	$Cd(NO_3)_2.4H2O$	Solid	SD Fine-Chem Ltd.
11	Aluminium Nitrate	$Al(NO_3)_3.9H_2O$	Solid	SD Fine-Chem Ltd.
12.	Sodium chloride	NaCl	Solid	SD Fine-Chem Ltd.
13	Potassium permanganate	$KMnO_4$	Solid	Sigma Aldrich
14	Mercuric Nitrate	$Hg(NO_3)_2.H_2O$	Solid	SD Fine-Chem Ltd.
15	Cupric nitrate	$Cu(NO_3)_2.3H_2O$	Solid	SD Fine-Chem Ltd.
16	Ethanol	C_5H_5OH	Liquid	Sigma Aldrich
17	Magnesium Chloride	$MgCl_2$	Solid	SD Fine-Chem Ltd.
18	Isopropyl alcohol (IPA)	C_3H_7OH	Liquid	SD fine-chem Ltd.
19	Thiourea	C_3H_6S	Solid	SD fine-chem Ltd.
20	Glucose	$C_6H_{12}O_6$	Solid	Sigma Aldrich
21	Sulfuric acid	H_2SO_4	Liquid	Sigma Aldrich
22	Methanol	CH_3OH	Liquid	SD fine-chem Ltd.
23	Phosphoric acid	H_3PO_4	Liquid	Sigma Aldrich
24	Ascorbic Acid	$C_6H_8O_6$	Solid	Sigma Aldrich
25	Sodium hydroxide	NaOH	Solid	SD Fine-Chem Ltd.
26	Sodium acetate	$C_2H_3NaO_2$	Solid	SD Fine-Chem Ltd.
27	Nitric Acid	HNO_3	Liquid	SD Fine-Chem Ltd.
28	Hydrogen peroxide	H_2O_2,	Liquid	Sigma Aldrich
29	Hydrochloric acid	HCl	Liquid	SD Fine-Chem Ltd.
30	2,4,6-Trinitrophenol	$C_6H_3N_3O_7$	Solid	Sigma Aldrich
31	2-chlorophenol	C_6H_5ClO	Solid	Sigma Aldrich
32	4-nitrophenol	$C_6H_5NO_3$	Solid	Sigma Aldrich
33	Phenol	C_6H_5OH	Solid	Sigma Aldrich
34	1,3-dinitrobenzene	$C_6H_4(NO_2)_2$	Solid	Sigma Aldrich
35	Bromobenzene	C_6H_5Br	Liquid	Sigma Aldrich
36	Nitrobenzene	$C_6H_5NO_2$	Liquid	Sigma Aldrich
37	Iodobenzene	C_6H_5I	Liquid	Sigma Aldrich
38	Resorcinol	$C_6H_4(OH)_2$	Solid	Sigma Aldrich
39	2,4-dinitrophenylhydrazine	$C_6H_6N_4O_4$	Solid	Sigma Aldrich
40	Aniline	$C_6H_5NH_2$	Liquid	Sigma Aldrich
41	4-nitroaniline	$C_6H_6N_2O_2$	Solid	Sigma Aldrich
42	2-nitrophenol	$C_6H_5NO_3$	Solid	Sigma Aldrich
43	Thiosemicarbazide	CH_5N_3S	Solid	Sigma Aldrich
44	Potassium Chloride	KCl	Liquid	Merck
45	Acetone	$(CH_3)_2CO$	Liquid	SD Fine-Chem Ltd.
46	Quinine sulphate	C40H50N4O8S	solid	Sigma Aldrich
47	Tetramethylbenzidine (TMB)	$C_{16}H_{20}N_2$	Solid	Sigma Aldrich
48	Terephthalic acid	C_6H_4-1,4-$(CO_2H)_2$	solid	Sigma Aldrich
49	Glycine (Gly)	$C_2H_5NO_2$	Solid	Sigma Aldrich
50	Valine (Val)	$C_5H_{11}NO_2$	Solid	Sigma Aldrich

51	Alanine (Ala)	$C_3H_7NO_2$	Solid	Sigma Aldrich
52	Proline (Pro)	$C_5H_9NO_2$	Solid	Sigma Aldrich
53	Leucine (Leu)	$C_6H_{13}NO_2$	Solid	Sigma Aldrich
54	Lysine (Lys)	$C_6H_{14}N_2O_2$	Solid	Sigma Aldrich
55	Isoleucine (Ile)	$C_6H_{13}NO_2$	Solid	Sigma Aldrich
56	Serine (Ser)	$C_3H_7NO_3$	Solid	Sigma Aldrich
57	Threonine (Thr)	$C_4H_9NO_3$	Solid	Sigma Aldrich
58	Glutathione (GSH)	$C_{10}H_{17}N_3O_6S$	Solid	Sigma Aldrich
59	Phenylalanine (Phe)	$C_9H_{11}NO_2$	Solid	Sigma Aldrich
60	Tryptophan (Trp)	$C_{11}H_{12}N_2O_2$	Solid	Sigma Aldrich
61	Tyrosin (Tyr)	$C_9H_{11}NO_3$	Solid	Sigma Aldrich
62	Methionine (Met)	$C_5H_{11}NO_2S$	Solid	Sigma Aldrich
63	Cysteine (Cys)	$C_3H_7NO_2S$	Solid	Sigma Aldrich
64	Glutamic acid (Glu)	$C_5H_9NO_4$	Solid	Sigma Aldrich
65	Arginine (arg)	$C_6H_{14}N_4O_2$	Solid	Sigma Aldrich
66	Glutamine (Gln)	$C_5H_{10}N_2O_3$	Solid	Sigma Aldrich
67	Aspartic acid (asp)	$C_4H_7NO_4$	Solid	Sigma Aldrich
68	Asparagine (asn)	$C_4H_8N_2O_3$	Solid	Sigma Aldrich
69	Methyl alcohol (MA)	CH_3OH	Liquid	SD fine-chem Ltd.
70	Dimethyl sulfoxide (DMSO)	$(CH_3)_2SO$	Liquid	SD fine-chem Ltd.
71	Dulbecco's Modified Eagle's medium	*******	liquid	Invitrogen Corporation
72	Fetal bovine serum	*******	liquid	Gibco
73	Penicillin	*******	liquid	Gibco
74	Streptomycin	*******	liquid	Gibco
75	HeLa cervical cancer cells	*******	liquid	American Type Culture Collection (ATCC)
76	Citric acid	$C_6H_8O_7$	Solid	Sigma Aldrich
77	Acetylcholinesterase	*******	*******	Sigma Aldrich
78	Acetylthiocholine	*******	*******	Sigma Aldrich
79	5, 5-dithiobis(2-nitrobenzoic acid)	$C_{14}H_8N_2O_8S_2$	Solid	Sigma Aldrich
80	Chlorpyrifos	$C_9H_{11}Cl_3NO_3PS$	Solid	Sigma Aldrich
81	Profenofos	$C_{11}H_{15}BrClO_3PS$	Liquid	Sigma Aldrich
81	Malathion	$C_{10}H_{19}O_6PS_2$	Solid	Sigma Aldrich
82	Glyphosphate	$C_3H_8NO_5P$	Solid	Sigma Aldrich

2.3 Methods

2.3.1. Synthesis of carbon quantum dots (CQDs)

Hydrothermal treatment has been used to synthesize CQDs from chemical and natural organic precursors. Typically, CQDs are synthesized by dispersing precursors in ultrapure water, sealing them in a Teflon-lined stainless steel autoclave, and then heating them at high temperatures for 3-5 hours. To remove the larger and agglomerated particles, the obtained dark brown solution was filtered and centrifuged at 10,000 rpm for 15 minutes at room temperature. To obtain pure CQDs, the obtained supernatant was filtered against a dialysis membrane and a syringe filter. As part of the experimental section, chapters 3, 4, and 5 describe the details of the CQD synthesis procedure.

2.4 Preparation of standard

The standard solution of ascorbic acid, TMB, PA and chlorpyrifos were prepared in organic solvent and distilled water. Prepared standard stock solution were stored at 5°C.

2.4.1. Preparation of standard solution of ascorbic acid (AA)

In a volumetric flask, 20 mg of ascorbic acid was dissolved in 10 mL of distilled water to prepare the stock solution of ascorbic acid with a concentration of $1x\ 10^{-2}$ M. A serial dilution of the stock solution was used to prepare the lower concentration of ascorbic acid solution.

2.4.2. Preparation of standard solution of 3,3′,5,5′-Tetramethylbenzidine (TMB)

We prepared a stock solution of TMB with a concentration of $1x\ 10^{-2}$ M by dissolving 24.0 mg of TMB in 10 mL of ethanol. TMB stock solution was serially diluted in ethanol to obtain the desired concentration.

2.4.3. Preparation of standard solution of Picric Acid (PA)

To prepare a stock solution of PA with a concentration of $1x\ 10^{-2}$ M; 23 mg of $C_6H_3N_3O_7$. In a volumetric flask, 10 mL of distilled water were dissolved in H_2O. Serial dilutions were used to obtain the desired concentration of PA solution from stock solution.

2.4.4. Preparation of standard solution of chlorpyrifos

The stock solution of chlorpyrifos with concentration of 1x 10^{-2} M was prepared by dissolving 35.0 mg of $C_9H_{11}Cl_3NO_3PS$ in 10 mL of distilled water in volumetric flask. To obtained desired concentration serial dilution technique was utilized. The stock solution of other pesticides were prepared in similar manner by dissolving appropriate quantity of each pesticides in distilled water separately.

2.5 Biocompatibility and Cell Viability studies

The cell viability or cytotoxicity of CQDs were investigated through MTT assay on different cell line according to a standard protocol. The detail experimental procedures and results are mention in chapter 4.

2.6 Calculations

2.6.1. Quantum yield (QY) determination

Quantum yields were also studied with quinine sulphate as a standard solution (QY = 54% at 360 nm). The 0.1M H_2SO_4 solution of quinine sulphate was measured for absorbance (below 0.1) and fluorescence spectrum was performed and fluorescence integrated intensity was calculated. A similar measurement was performed on fluorescent material, and the quantum yield was determined using equation 2.1.

$$QY = QY_s.\frac{I}{I_s}.\frac{A_s}{A}.\frac{\eta^2}{\eta_s^2} \qquad 2.1$$

The QY stands for the quantum yield, the I stands for the integrated fluorescence emission intensity, the A stands for the optical density, the η stands for the refractive index of the solvent (for the ultrapure water as solvent, the $\eta/\eta_s = 1$), and the s stands for the standard.

2.6.2. Determination of limit of detection (LOD)

The limit of detection (LOD) is the least concentration of hazardous materials, measured based on a certain level of confidence. In order to calculate it, use the formula below

$$LOD = 3\sigma/s \qquad 2.2$$

Where, "σ" is the standard deviation of the blank and "s" is the slope of the calibration sensitivity.

2.6.3. Determination of Stern-Volmer constant

This equation was used to calculate the Stern-Volmer quenching constant

$$(F_0/F)-1 = K_{sv}[Q] \qquad 2.3$$

Where "F" is the fluorescence intensity of sensor in the presence of analyte and "F_0" is the fluorescence intensity of sensor. "K_{sv}" is the Stern-Volmer quenching constant and "[Q]" is the concentration of quencher.

2.7 Characterization of CQDs

2.7.1. Transmission Electron Microscopy (TEM)

This technique can be used to analyse morphology, defects, crystallographic structure, particle size, and even composition of a specimen. In this technique, a beam of electrons is passed through an ultra-thin specimen, interacting with the sample as it passes. As electrons travel through a specimen, an image is formed. The image is magnified and focused on an imaging device, such as a fluorescent screen, a photographic layer, or a sensor, such as a CCD camera to be detected as shown in **figure 2.1**. It works on the same principles as the light microscope, but uses electrons rather than light. Light microscopes are limited by their wavelength, which determines the type of image that can be observed. By using electrons as their "light source", TEM provides a resolution a thousand times higher than that of a light

microscope. Due to the small De Broglie wavelength of electrons, TEM can image at a much higher resolution than light microscopes. In this manner, a user of the instrument is able to examine detail even down to the smallest atom, which is tens of thousands of times smaller than the smallest resolvable object in a light microscope. A range of scientific fields, including physical and biological sciences, utilize TEM as an analysis method. TEMs are used in cancer research, virology research, materials science research, and pollution research. At smaller magnifications, TEM image contrast is caused by absorption of electrons in the material due to its thickness and composition. Higher magnifications result in complex wave interactions that modulate the image intensity, making expert interpretation of observed images necessary. As well as regular absorption-based imaging, the TEM may also observe modulations in chemical identity, crystal orientation, electronic structure, and sample-induced electron phase shift as shown in **figure 2.2.**

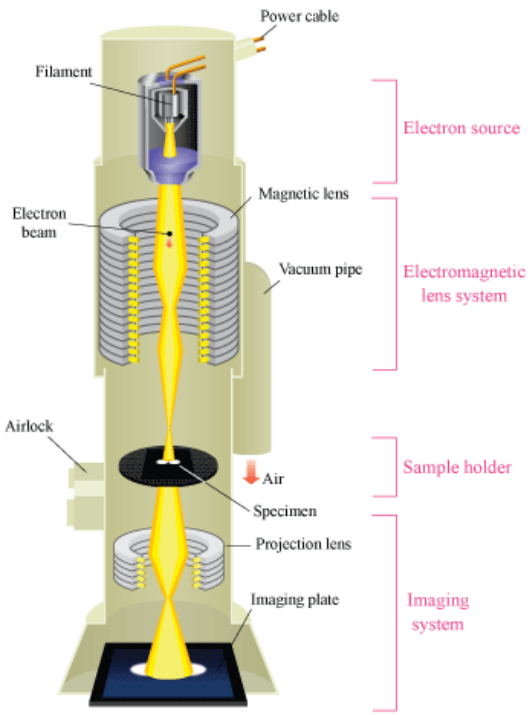

Figure 2.1 Schematic representation of working of TEM

Figure 2.2 Photograph of Transmission electron microscopy (TEM).

2.7.2. Fourier Transform Infra-Red Spectroscopy (FT-IR)

A Fourier transform infrared (FT-IR) spectrometer is one of the most versatile techniques used to analyse organic compounds in both a qualitative and quantitative manner, providing information on molecular structure, chemical bonds, and molecular environment. Additionally, it is used to determine the presence of different functional groups in compounds and molecules. In the FT-IR system, the working principle is based on Michelson interferometers consisting of beam splitters, fixed mirrors, and movable mirrors that move back and forth. In the beam splitter, the radiation from the source is split into two beams. During a beam splitter operation, one beam travels to a static mirror, while a second beam is reflected from the beam splitter to a moving mirror. Radiation is reflected back to the beam splitter by the fixed and moving mirrors. The beam splitter reflects half of this reflected radiation and transmits the other half, so that one beam passes through the sample, is detected by a detector,

and spectra are displayed on the computer, and the other beam returns to the source as shown in **figure 2.3.**

An FT-IR spectra was recorded of the sample in the present study with the instrument "PerkinElmer Spectrum 100" at room temperature along with mid-infrared radiation sources. Spectra were displayed in transmitted mode after radiation sources passed through the KBr window and transmitted data was collected by $LiTaO_3$ detector. KBr was mixed with the sample in a ratio of 1:100 to prepare the pellets and the pellets were scanned in the range of 400-4000 cm^{-1} with a spectral resolution of 4.0 cm^{-1} and a scanning speed of 0.2 cm/sec.

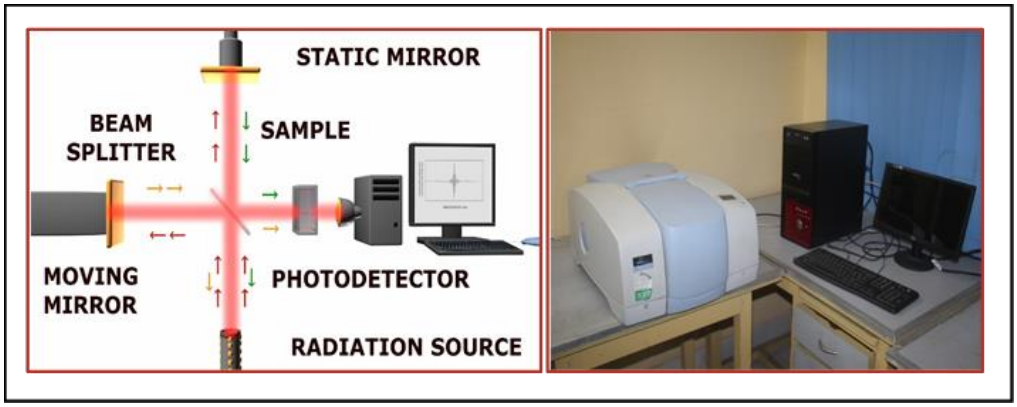

Figure 2.3 Illustration of the FT-IR process and its photographs

2.7.3. UV-visible Spectroscopy

UV-visible spectroscopy involves studying the interactions of light with chemical molecules. Through a chemical compound, light is absorbed, transmitted, and reflected over a certain range of wavelengths. The spectrophotometry technique measures the amount of light absorbed or transmitted by chemical compounds. Transmittance is defined as the ratio of the intensity of light entering the sample (I_0) to the intensity of light exiting the sample (I_t) at a particular wavelength and expressed as a percentage (%T) (**Equation 2.4**).

$$\%T = \left(\frac{I_0}{I_t}\right) \times 100 \qquad 2.4$$

In **Equation 2.5**, the absorbance (A) is the negative logarithm of the transmittance.

$$A = -\log T \qquad 2.5$$

The UV-visible region of electromagnetic radiation ranges from 190 to 700 nm. The two most important laws of absorption analysis are Beer's laws and Lambert's. Beer's law states that absorption is proportional to concentration of absorbing molecules, and Lambert's law states that the fraction of radiation absorbed is independent of the intensity of the radiation. Beer-Lambert's Law (**Equation 2.6**) results from combining these two laws.

$$\log_{10}\left(\frac{I_0}{I_t}\right) = \varepsilon c l \qquad 2.6$$

"I_0" represents the intensity of an incident radiation and "I_t" denotes the intensity of the transmitted radiation, and 'ε' symbolises the molar absorption coefficient, which is fixed for every absorbing material, and "l" represents the path length and "c" represents the concentration of the absorbing molecule. The non-bonding (lone pair electrons) orbitals are higher in energy compared to the π bonding orbitals, which are higher in energy than the σ bonding orbitals. An electromagnetic field with the correct frequency absorbs electromagnetic radiation, transitioning from one of these orbitals to an empty orbital, i.e. σ* or π*.The energy differences between orbitals depend on the bonding system and the atoms present. Most transitions from bonding orbitals have too short a wavelength (too high a frequency) to be easily measured.

In analytical chemistry, UV-visible spectroscopy is used to quantify analytes such as transition metal ions, conjugated organic compounds, and biological macromolecules. As a result of UV-visible radiation absorption, the nonbonding electrons are excited and go to higher antibonding orbitals and there are four possible transitions: σ–σ* > n–σ* > π–π* > n–π*. The most common transition occurs in the π-conjugated and nonbonding molecules are shown in **figure. 2.4** with the examples of π→π*, n→σ* and n→π*.

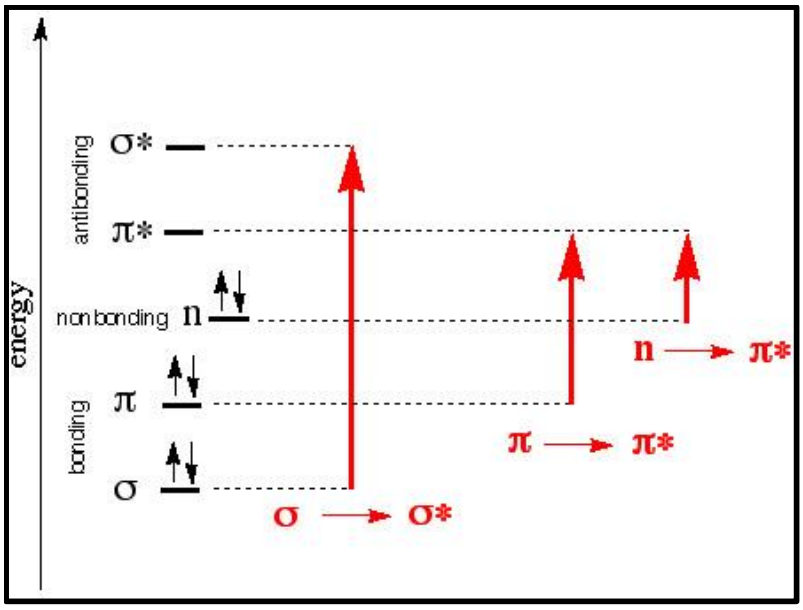

Figure 2.4 Schematic of Possible Electronic Transitions in UV-visible Spectroscopy

There are numerous components of an UV-visible spectrophotometer, such as light sources (UV and VIS), monochromators (wavelength selectors), sample holders, detectors, signal processors, and readouts. For UV-regions, deuterium arc lamps are often used and for visible regions, tungsten lamps. The UV-visible absorption spectra of the synthesized materials were obtained with "Evaluation 201 Thermo Scientific" by using quartz cuvettes with a path length of 1 cm in the wavelength range of 200–700 nm. A schematic diagram and photograph of the UV-visible spectrophotometer are shown in **Figure 2.5.**

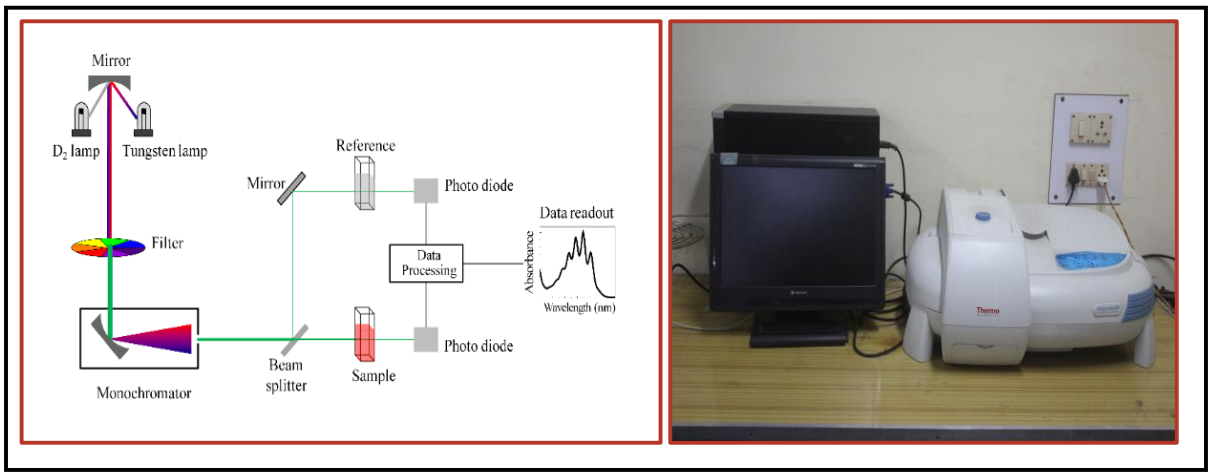

Figure 2.5 Illustration of working principle and photograph of UV-visible spectroscopy

2.7.4. Fluorescence Spectroscopy

Fluorescence occurs when photons stimulate a molecule to become electrically excited by photons. It is caused by the absorption of photons in the singlet ground state being promoted to a singlet-excited state. The excited molecule returns to ground state by emitting an energy-lower photon with a longer wavelength than the photon absorbed. The fluorescence spectroscopy technique is one of the most versatile, non-destructive, and sensitive ways to obtain information about a material's electronic structure. An emission spectrophotometer measures the emission intensity and spectral content of a sample. This is a direct measure of various important properties of the sample, such as defects or impurities, and the magnitude of the intensity allows their concentration to be determined. Furthermore, during fluorescence recording, the excitation, emission, or both wavelengths may be scanned and the change of signal with temperature, time, polarization, and concentration can be monitored. The fluorescence spectrum differs from the absorption spectrum in that the absorption spectrum measures transitions from the ground state to the excited state, whereas the fluorescence spectrum measures transitions from the excited state to the ground state. The fluorescence spectrum is a plot of emission intensity versus excitation wavelength. The wavelength at which a molecule shows maximum absorbance can be used as an excitation wavelength, resulting in a longer wavelength emitting more light at a value usually twice that of the excitation wavelength. The schematic diagram of the key component of the fluorescence spectrometer is shown in **figure 2.6.**

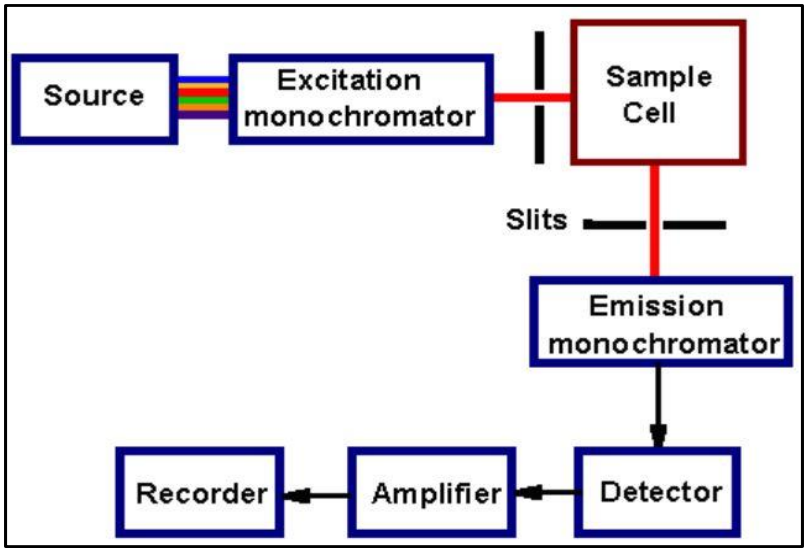

Figure 2.6 Fluorescence spectrophotometer working principle diagram.

Spectra of fluorescence were recorded using two different Fluorescence Spectrophotometers (Fluoromax 4, Horiba USA), and Varian Cary Eclipse Fluorescence Spectrophotometers **(Figure 2.7).**

Figure 2.7 A photo of a fluorescence spectrophotometer

2.7.5. X-ray Diffraction (XRD)

The X-ray diffraction technique determines grain size, atomic spacing, lattice parameters and degree of crystallinity in a mixture of amorphous and crystalline substances using a rapid, non-destructive analysis. The technique can be used for powder samples or thin

film samples of various materials. An X-ray source generates monochromatic radiation inside a cathode ray tube after which it is filtered to produce monochromatic radiation, collimated to focus, and directed toward a sample. The diffraction pattern is produced by constructive interference between incident X-rays and crystalline samples. A typical X-ray diffraction experiment involves cathode ray tubes that generate X-rays, and then collimating and directing the radiation toward the sample. The interaction of incident rays with the sample produces constructive interference, i.e. diffracted rays, when Bragg's law is satisfied. The diffracted X-rays are then detected, processed, and counted, and all possible diffraction directions of the lattice should be obtained since the powdered material is randomly oriented by scanning it over a range of 2θ angles.

The schematic illustration of X-ray diffraction by crystalline planes is shown in **figure 2.8.** XRD analysis of CQDs was achieved using a Rigaku MiniFlex 600 desktop X-ray diffractometer using Cu-Kα radiation, λ=1.5A˚ scanned at a scan rate of 5˚/min in the 2θ range of 5˚-80˚.

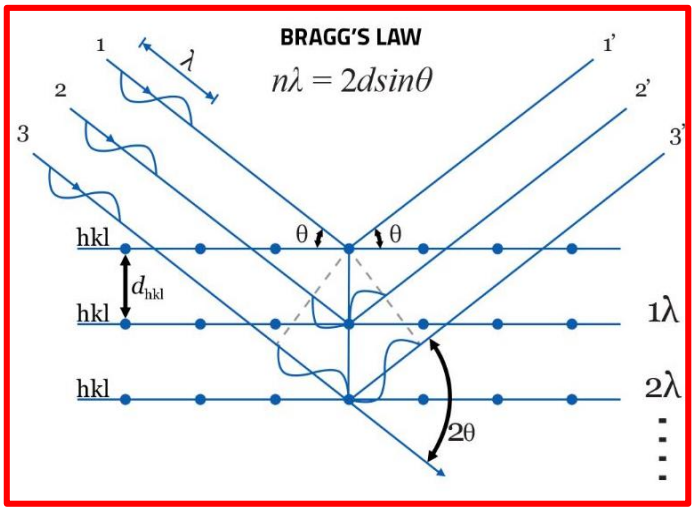

Figure 2.8 Schematic illustration of X-ray diffraction by crystal planes

2.7.6. Zeta Potential

Zeta potential is the difference in potential between the dispersion medium and the stationary fluid layer in contact with the dispersed particles. It is typically written as Greek letter zeta (ζ) and represented in units of volts (V) or millivolts (mV). The surface charge of nanoparticles is determined by the Zeta potential. The Zeta potential of colloidal nanoparticles is an important term describing their stability. Zeta potential measures the strength of electrostatic repulsion between adjacent particles with similar charges moving in a dispersion. Typically, zeta potentials range from +100 mV to -100 mV. Dispersion, aggregation, and flocculation are explained by the ζ potential. Therefore, colloids with high zeta potentials (negative or positive) tend to be electrically stabilized, whereas colloids with low zeta potentials tend to coagulate or flocculate. As a result, it can be used in the formulation of dispersions, emulsions, and suspensions. In Figure 2.16, the zetasizer's working principle is shown as well as a digital image of it. Malvern Zetasizer (Malvern Instruments, Ltd.) was used to measure the zeta potential CQDs.

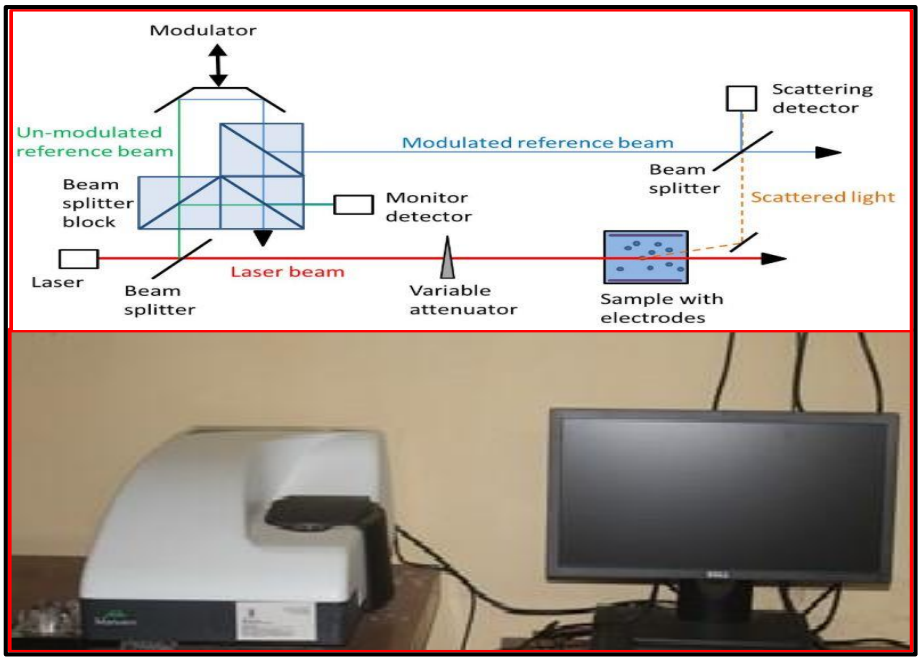

Figure 2.9. The working principle of Zetasizer and its photograph

2.7.7. X-ray Photoelectron Spectroscopy (XPS)

As the most widely used surface analysis technique, XPS or Electron Spectroscopy for Chemical Analysis (ESCA) is applicable to a wide range of materials and provides valuable quantitative and chemical state information. The advantage of XPS is that it is capable of not only showing which elements are within a sample, but also what other elements they are bound to. In an XPS measurement, the average depth of analysis is approximately 5 nm. In XPS analysis, target materials are irradiated with X-rays of sufficient energy in ultrahigh vacuum conditions around 10^{-9} millibar (mbar); this results in the excitation of electrons in specific bound states. As some of the photo-ejected electrons scatter inelastically through the sample, others undergo prompt emission and suffer no energy loss in escaping the surface and entering the surrounding vacuum. In the vacuum, these photo-ejected electrons are collected by an electroanalyser that measures their kinetic energy. In an electron energy analyzer, electron intensity is plotted against binding energy (the energy the electrons had before they left the atom) in relation to how many electrons are ejected over time. The prominent energy peaks on the spectrum correspond to specific elements. Peak intensities can also indicate the amount of each element in a sample. The peak area of each element is proportional to the number of atoms present in the element, and chemical composition is derived by calculating the contribution of each peak area. There are several components of an XPS system: an X-ray source, a monochromator, a stainless steel chamber with high vacuum pumps, an electron collection lens, an electron energy analyzer, an electron detector, and a sample introduction chamber with moderate vacuum **(Figure. 2.10).** It is common to use Al Kα or Mg Kα for the X-ray source.

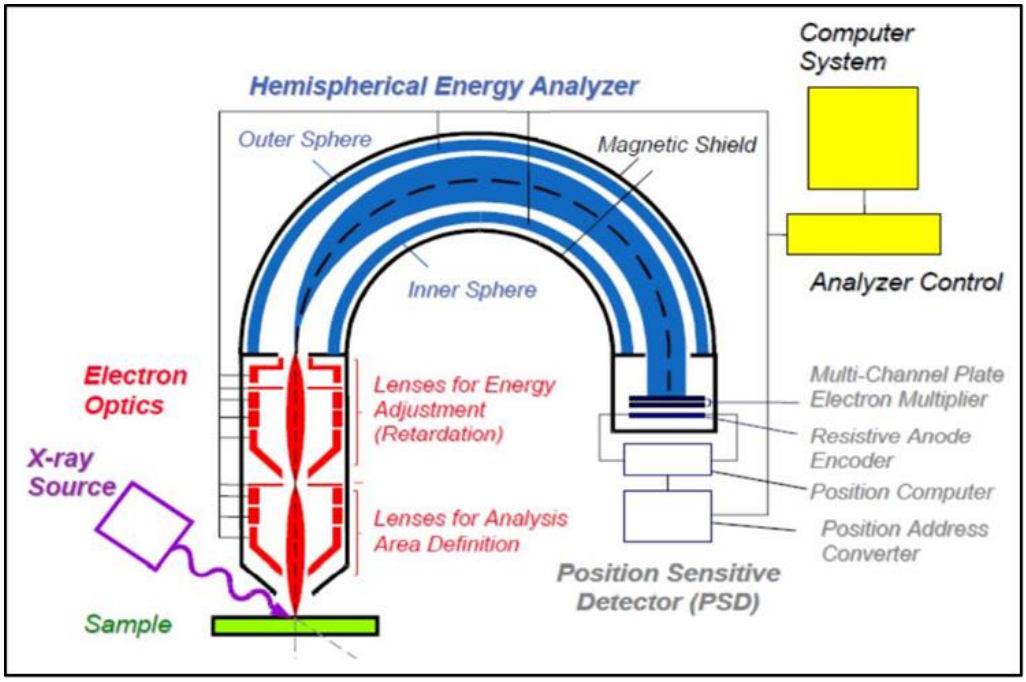

Figure 2.10. Working principle of X-ray photoelectron spectroscopy (XPS)

The XPS analysis was performed on an AMICUS, Kratos, Analytical, Shimadzu spectrometer using Mg Kα (1253.6 eV) radiation **(Figure. 2.11)** in the present study.

Figure 2.11. Typical photograph of XPS instrument